HHS Public Access

Author manuscript

Cell Signal. Author manuscript; available in PMC 2017 September 01.

Published in final edited form as:

Cell Signal. 2016 September ; 28(9): 1325–1335. doi:10.1016/j.cellsig.2016.05.013.

CSF-1 receptor signalling is governed by pre-requisite EHD1 mediated receptor display on the macrophage cell surface

Luke R. Cypher[1], **Timothy Alan Bielecki**[1], **Lu Huang**[4], **Wei An**[2], **Fany Iseka**[2], **Eric Tom**[3], **Matthew D. Storck**[1], **Adam D. Hoppe**[4], **Vimla Band**[1,2], and **Hamid Band**[1,2,*]

[1]Eppley Cancer Institute for Research in Cancer & Allied Diseases, University of Nebraska Medical Center, Omaha, Nebraska, United States of America

[2]Department of Genetics, Cell Biology, & Anatomy, University of Nebraska Medical Center, Omaha, Nebraska, United States of America

[3]Department of Biochemistry & Molecular Biology, University of Nebraska Medical Center, Omaha, Nebraska, United States of America

[4]Department of Chemistry and Biochemistry, South Dakota State University, Brookings, South Dakota, United States of America

Abstract

Colony stimulating factor-1 receptor (CSF-1R), a receptor tyrosine kinase (RTK), is the master regulator of macrophage biology. CSF-1 can bind CSF-1R resulting in receptor activation and signalling essential for macrophage functions such as proliferation, differentiation, survival, polarization, phagocytosis, cytokine secretion, and motility. CSF-1R activation can only occur after the receptor is presented on the macrophage cell surface. This process is reliant upon the underlying macrophage receptor trafficking machinery. However, the mechanistic details governing this process are incompletely understood. C-terminal Eps15 Homology Domain-containing (EHD) proteins have recently emerged as key regulators of receptor trafficking but have not yet been studied in the context of macrophage CSF-1R signalling. In this manuscript, we utilize primary bone-marrow derived macrophages (BMDMs) to reveal a novel function of EHD1 as a regulator of CSF-1R abundance on the cell surface. We report that EHD1-knockout (EHD1-KO) macrophages cell surface and total CSF-1R levels are significantly decreased. The decline in CSF-1R levels corresponds with reduced downstream macrophage functions such as cell proliferation, migration, and spreading. In EHD1-KO macrophages, transport of newly

*Correspondence: Hamid Band M.D., Ph.D., University of Nebraska Medical Center, DRC II – 5064, Omaha, NE 68198-5950, Tel: (402) 559-8572; Fax: (402) 559-4651; hband@umnc.edu.

Author Contributions

LRC conducted, designed, and analyzed the results of most of the experiments. HB conceived the study, designed experiments, and wrote the paper with LRC. VB conceived the study with HB. TB conducted western blotting and migration assays with LRC. LH and AH performed immunofluorescence for CSF-1R surface and total levels. MS and TB helped LRC with mouse husbandry. WA and FI edited the manuscript with LRC and HB.

Conflict of Interest

The authors declare no conflicts of interest.

synthesized CSF-1R to the macrophage cell surface was reduced and was associated with the shunting of the receptor to the lysosome, which resulted in receptor degradation. These findings reveal a novel and functionally important role for EHD1 in governing CSF-1R signalling via regulation of anterograde transport of CSF-1R to the macrophage cell surface.

Graphical Abstract

Working model of the EHD1 function in CSF-1R transport to the cell surface. EHD1-dependent post-Golgi sorting of newly synthesized CSF-1R in BMDMs directs the receptor towards the cell surface and away from the lysosome. In EHD1-expressing BMDMs, the surface delivery dominates. In the absence of EHD1, the lysosomal delivery is dominant, resulting in lower surface CSF-1R and reduced CSF-1R dependent cellular activation together with increased CSF-1R delivery to the lysosome for degradation.

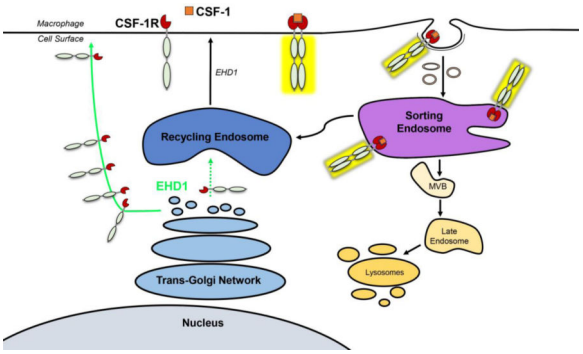

Keywords

CSF-1R; macrophage; proliferation; cell signalling; cell surface; receptor tyrosine kinase

1. Introduction

Cells of the monocyte-macrophage lineage play fundamental roles in integrating innate and adaptive arms of immune defense and aberrations of development or function of this cell lineage are incompatible with an effective immune system [1,2]. Macrophages are key contributors to highly prevalent immunological diseases [3–5] such as rheumatoid arthritis, inflammatory bowel disease, and demyelinating neurological diseases [6–8]. Macrophages also play key homeostatic roles in non-immune tissues and contribute to diseases such as atherosclerosis and cancer [9–11].

Colony-stimulating factor-1 receptor (CSF-1R) is a receptor tyrosine kinase (RTK) essential for macrophage development and physiological functions, such as cell proliferation, differentiation, spreading, migration, phagocytosis and cytokine secretion [12]. Similar to other RTKs, ligand binding of Colony-stimulating factor-1 (CSF-1) activates CSF-1R by inducing conformational changes, dimerization, and trans-phosphorylation, leading to association of key cytoplasmic signalling intermediates. This activates signal transduction cascades, including the PI3-kinase/AKT, Ras/Erk, and Rho/Rac pathways [13,14].

Ligand binding (RTK activation) induces the endocytic internalization of RTKs, and this has been demonstrated for CSF-1R [15–17]. Endocytosed RTKs are targeted to the lysosome, which we and others have established to be dependent on ubiquitination via CBL-family and recognition by ESCRT complexes [15,18–21]. Internalization and degradation of RTKs have classically been thought to be a mechanism for cellular attenuation of RTK signalling. However, activated RTKs are known to signal in endosomes and may require endocytosis to transduce specific signals [22]. Recently, Erk1/2 activation due to CSF-1R signalling has been shown to require endocytosis, while signalling at the cell surface was sufficient for STAT pathway activation [23].

Compared to intracellular trafficking of ligand-stimulated RTKs, the trafficking of unstimulated/basal RTKs is less understood. In the absence of CSF-1, CSF-1R has been shown to undergo constitutive internalization and basal recycling at a relatively low rate [24]. An understanding of the mechanisms of RTK traffic in the absence of ligand-induced activation is of fundamental importance as these mechanisms, together with the anterograde transport of newly synthesized protein, help determine the level of the activation-ready, cell surface pool of RTKs. Such mechanisms can also determine the kinetics of restoration of cell surface RTK display following ligand-induced degradation for subsequent ligand binding and activation. Yet, little is known about these basic mechanisms of RTK traffic, and CSF-1R trafficking in macrophages has not been reported.

The four members of the Eps15-homology domain-containing (EHD) protein family have emerged as regulators of cellular receptor trafficking [25]. Structurally, EHD proteins are characterized by highly related primary amino acid sequences and conserved domain structure amongst family members: a nucleotide-binding G-domain that folds similarly to the GTPase dynamin, but instead hydrolyzes ATP; coiled-coiled regions that form a membrane lipid-binding domain; and an EH domain near the C-terminus that mediates interactions with partner proteins by binding to asparagine-proline-phenylalanine (NPF)-containing motifs [26]. *In vitro* studies have established that EHD proteins function similarly to dynamin as scission proteins to promote vesicular budding involved in cellular trafficking of receptors [27]. While biochemical roles of EHD proteins have been elucidated in some detail, their physiological roles are just now being unraveled.

Our laboratory has previously utilized mouse models to understand the physiological functions of EHD family proteins [28–34]. We have found that EHD1 deletion on a mixed C57BL/6 and 129Sv background is partially penetrant embryonic lethal and associated with defective spermatogenesis and lens developmental defects, while it is fully embryonic lethal on a predominantly C57BL/6 background [35–37]. Here, we use primary bone marrow-derived macrophages (BMDMs) with inducible EHD1-Knockout (EHD1-KO) capacity, to study the biological and physiological function of EHD1 in macrophages. Here, we report EHD1 is required for delivery and display of CSF-1R upon the cell surface, ensuring CSF-1R activation/signalling, and downstream macrophage functional response.

2. Materials & Methods

2.1 Reagents & Antibodies

Bovine Serum Albumin (cat. # A7906-100G), Paraformaldehyde (cat. # 158127-500G), Triton X-100 (cat. # 93418), and 4-hydroxytamoxifen (cat. # T176-10MG) were from Sigma-Aldrich (St. Louis, MO). Propidium Iodide staining solution (cat. # 00-6990-42) was from eBiosciences. Hema staining solutions (cat. # 23-123919) were from Fisher. 3H-thymidine (cat. # 2407001, 2.0Ci/mmol) was from MP Biomedical and [35S] (cat. # NEG772007MC, 1175 Ci/mmol) was from Perkin Elmer. Bafilomycin A1 (cat. # 196000) was from MilliPore. EDTA-free protease inhibitor cocktail (cat. # 4693159001) was from Roche, ECL development reagent (cat. # 32106) was from Thermo-Scientific. Recombinant CSF-1 (catalog # 315-02) was from Peprotech (Rocky Hill, NJ). CFSE (cat. # C34554), RPMI-1640 (cat. # SH30027.02). Penicillin/streptomycin (cat. # 15140-122) and Fetal Bovine Serum (cat. # 10427-028; lot # 1662765A120-01) were from Life Technologies. Antibodies: Brilliant Violet 711 conjugated anti-CSF1R and anti-CSF1R, AFS98 (cat. # 135515) were from Biolegend; anti-CSF1R C-20 (cat. # sc-692), anti-CSF1R G-17 (cat. # sc-31638) anti-HSC70 (cat. #sc-7298), and anti-LAMP1 1D4B (cat. # sc-19992) were from Santa Cruz Biotechnology; anti-EHD1 (cat. # ab109311) was from Abcam; anti-ß-Actin (cat. # A5316) was from Sigma-Aldrich; anti-pErk42/44 (cat. # 9101) and P-M-CSF Receptor (Y723, 49C10) was from Cell Signaling Technology; F4/80-APC, BM8 (cat. # 17-4801-82), anti-GM130 (cat. # 610822), CD16/32 (cat. # 14-0161), and APC-conjugated anti-Annexin V (cat. # 17-8007-72) were from eBiosciences; a polyclonal rabbit antibody recognizing EHD1 and EHD4 was generated in-house was described previously (45). Secondary fluorochrome-conjugated antibodies were from Life Technologies.

2.2 Mice Generation & Genotyping

Ehd1$^{fl/fl}$ mice in a predominantly C57BL/6 background [37,38] were crossed with tamoxifen-inducible CreERT2 expressing mice from Jackson Laboratories (*Gt(ROSA)26Sor*$^{tm1(cre/ERT2)Tyj}$; strain 008463) to generate *Ehd1*$^{fl/fl}$; *Cre*^{ERT2} mice. Genotypes were confirmed by subjecting tail clip DNA to PCR analysis using the KAPA mouse genotyping kit (KAPA Biosystems) and primers pairs described previously [36,38]. Mice were treated humanely according to the National Institutes of Health (NIH) and The University of Nebraska Medical Center guidelines. Animal studies were pre-approved by the Institutional Animal Care and Use Committee (#07-061-FC12).

2.3 Bone marrow derived macrophage culture (BMDMs)

Bone marrow was harvested from 8-12 week old mice by removing the femur bones, cutting the ends, and flushing with ice-cold PBS. Red blood cells where lysed with solute-free H_2O and the bone marrow was plated on tissue culture coated dishes for 16 hours to allow mature/non-progenitor cells to attach. The non-adherent progenitor population was collected by pipetting and re-plated in 15-cm petri dishes (non-tissue culture treated). Cells were then incubated for 6 days in BMDM media (RPMI w/ 15% FBS, 10% L929 supernatant [39] or 30 ng/ml recombinant CSF-1 and 1% penicillin/streptomycin) at 37°C and 5% CO_2, with change of medium every 2 days. To assess the impact of EHD1 deletion, *Ehd1*$^{fl/fl}$; *Cre*^{ERT2} BMDMs were either cultured in regular medium (control/wildtype EHD1 expression) or

medium containing 200 nM 4-hydroxytamoxifen (TAM) for 4 days to induce EHD1 deletion. This protocol was based on initial time course and titration studies to determine optimal culture conditions.

2.4 Fluorescence Activated Cell Sorting (FACS)

BMDMs were washed with ice-cold PBS and blocked for 10 minutes for non-specific binding with CD16/32 (Fc Blocker) and then incubated with appropriate antibodies at a dilution of 1:400 and put in the dark and on ice for 30min. Cells were then pelleted, washed with PBS twice, and suspended in 400 μl of 0.1% BSA/PBS, put on ice, and protected from light.

2.5 Quantitative real-time-PCR (qRT-PCR)

RNA was isolated from BMDMs grown on 10-cm tissue culture plates using Trizol reagent, and 1 ug of total RNA was reverse transcribed using the QuantiTect Reverse Transcription Kit (QAIGEN). 10% volume of the RT reaction of the ensuing cDNA was used with QuantiTect SYBR Green qRT-PCR Kit (QAIGEN) for quantitative qRT-PCR of mouse CSF-1R using the primer sequences (5'-3'): GCAGTACCACCATCCACTTGTA; GTGAGACACTGTCCTTCAGTGC. GAPDH was used as a control, and changes in CSF-1R were calculated using the cycle threshold method [40]. Each reaction was performed in triplicate in a volume of 50 uL with primers at a final concentration of 250 nM.

2.6 ^{3} H-thymidine incorporation assay

BMDMs were deprived of CSF-1 for 16 hours and plated in 48-well tissue culture plates at 1×10^{4} cells/well and allowed to attach overnight at 37 °C, 5% CO2. Cells were then treated with 30 ng/ml CSF-1 and allowed to proliferate for 2, 4 or 6 days. Cells were pulsed with 4μCi/well of ^{3}H-Thymidine for the last 6 hours of the assay. Radioactivity incorporated into DNA was collected by washing the cells with 10% TCA per well followed by 300μl per well 0.2 N NaOH at room temperature to dissolve DNA. Each sample was transferred into vials with 5 mL of scintillation fluid and counts per minute (c.p.m.) were recorded with a scintillation counter.

2.7 CFSE dye dilution assay

Macrophages were cultured with recombinant CSF-1 (30 ng/mL) for 2, 4 or 6 days after initial CFSE population staining (Day 0) according to ThermoFisher Scientific's protocol. Dilution of CFSE fluorescence as an indicator of cell division was assessed via Fluorescence Activated Cell Sorting (FACS) analysis The CFSE geometric mean fluorescence intensity (MFI) was used to access the degree of CSF1-induced cell division.

2.8 Microscopy & Imaging

Imaging using immunofluorescence was performed as previously described [41] with minor modifications. BMDMs were grown on glass coverslips and fixed with 2% PFA/PBS for 5 min. To assess the intracellular pools of CSF-1R, the cells were fixed and permeabilized in methanol for 10 minutes at −20°C. The cells were then blocked with 1:400 CD16/32 (Fc Blocker) in 1% BSA/PBS for 30 minutes and incubated with primary antibodies in 1%

BSA/PBS overnight. After 3 washes in PBS, the cells were incubated with the appropriate fluorochromeconjugated secondary antibody for 45 minutes at room temperature, washed and mounted using Fluoromount-G (Southern Biotech, Cat. # 0100-01) or VECTASHEILD mounting medium (Vector laboratories, Cat. # H-1400 and H-1500). Images were acquired using a LeicaCTR4000 inverted microscope equipped with an QICAM 12-bit color camera, 12V 100 W halogen lamp, QCapture software and 60x oil immersion lens (For CSF-1R) and a Zeiss 710 Meta Confocal Laser Scanning microscope (Carl Zeiss) using a 63× objective with a numerical aperture of 1.0 and appropriate filters. Merged fluorescence pictures were generated and analyzed using ZEN® 2012 software from Carl Zeiss.

2.9 Macrophage spreading assay

BMDMs cultured without (Control) or with (EHD1-KO) TAM were plated on coverslips and allowed to attach for 2 days. The cells were then deprived of CSF-1 for 16 hours and subsequently stimulated with 100ng/mL CSF-1 for 10 minutes. Cells were fixed for 10 minutes with 4% PFA, washed with PBS 3 washes for 10 minutes, and stained using conjugated Alexa Fluor® 594 Phalloidin (ThermoFisher Scientific). ImageJ software was used to quantify the surface area of macrophages.

2.10 Macrophage trans-well migration assay

BMDMs were deprived of CSF-1 for 4 hours and placed in the upper chambers of 5μm pore inserts (Corning, cat. # 3421) at 1×10^5 cells per chamber in 100μl RPMI without CSF-1. Cells were then allowed to migrate towards CSF-1 in the lower chamber (30 ng/ml) for 3 hours at 37°C. Cells on the lower surface of membranes were fixed with 100% methanol and stained with HEMA for 5 minutes. Cells were visualized under a bright field microscope. Migrated cells were counted in 10 fields per insert and the total number of migrated cells was calculated for control and EHD1-KO BMDMs.

2.11 Western blotting

Western blotting was performed as described [38]. Briefly, BMDMs were washed with ice-cold PBS and lysed in ice-cold Triton X-100 lysis buffer (0.5% Triton X-100, 50 mM Tris pH 7.5, 150 mM sodium chloride, and EDTA-free protease inhibitor cocktail). The lysates were vortexed, centrifuged at 13,000 rpm for 30 minutes at 4° C, and supernatants collected. Protein quantification was done using the Bicinconic acid (BCA) assay 40 μg of lysate protein per sample was resolved by SDS/PAGE and transferred to a PVDF membrane. The membranes were blocked in TBS/1% Bovine Serum Albumin (BSA), incubated with the appropriate primary antibodies diluted in TBS-0.1% tween 20 overnight at 4°C and washed in TBS-0.1% tween (3x for 10 minutes) followed by a 1-hour incubation with HRP-conjugated secondary antibody at room temperature. The membrane was then washed in TBS-0.1% tween (3x for 10 minutes each) and ECL-based detection performed.

2.12 [^{35}S]-methionine/cysteine metabolic labeling and Immunoprecipitation CSF-1R

BMDMs were seeded at 5×10^6 cells/10-cm plate in CSF-1 containing medium and cultured for 16 hours. The cells were washed and incubated in methionine/cysteine-free RMPI-1640 medium supplemented with 15% FBS and 30 ng/mL recombinant CSF-1 for 30 minutes at

37°C and pulsed with 0.1 mCi of [^{35}S] for 15 minutes at 37°C. Cells were then washed and incubated with regular culture medium containing a 20-fold excess of unlabeled methionine/cysteine for 0, 15, 30, and 60 minutes of chase. Cells were rinsed with ice-cold PBS and lysed in ice-cold Triton X-100 lysis buffer with EDTA-free protease inhibitor cocktail. Anti-CSF-1R immunoprecipitations were carried out using 500 μg samples of cleared lysate protein and anti-CSF-1R antibody followed by capture with Protein-A Sepharose beads. Samples were resolved by SDS/PAGE (8% gel). Gels were fixed, dried, and incubated with Auto-Fluor to amplify [^{35}S] signals and autoradiography was performed at −80°C in metal cassettes with intensifying screens.

2.13 Statistics

Unpaired student's *t* tests were used to calculate *p*-values. Data is presented as mean ± SEM, $p<0.05$ defines the threshold of statistical significance.

3. Results

3.1 EHD1-KO diminishes CSF-1R signalling in BMDMs

To determine if deletion of EHD1 had a functional impact in BMDMs, we first assessed whether or not EHD1-KO bone marrow progenitors maintained the ability to differentiate into mature macrophages (i.e. F4/80$^+$). *EHD1*$^{fl/fl}$; *CreERT2* BMDMs grown in the absence or presence of TAM were stained with F4/80 antibody and analyzed with FACS. Greater than 99% of both (−) and (+) TAM treated populations stained positively for F4/80$^+$ (Suppl. Fig. 1A), demonstrating the ability of these cells to differentiate into mature macrophage. We next performed toxicity controls to verify that any phenotypic effects observed in tamoxifen-induced EHD1-KO BMDM was a *bona fide* effect of EHD1 deletion and not an effect of tamoxifen treatment (Suppl. Fig. 1B-D). These assays showed tamoxifen did not attenuate CSF1-induced CSF-1R signalling responses in BMDMs. To assess the function of EHD1 in macrophage CSF1-induced cellular responses, we assayed the effects of CSF1-induced proliferation on control and EHD-KO BMDMs using two independent methods: ^{3}H-thymidine incorporation and CFSE dye dilution assays. These two assays have been previously used to assess CSF1–induced macrophage proliferation [54, 55]. Both assays showed EHD1-KO macrophages had significantly reduced proliferative responses when stimulated with CSF-1 (Fig. 1A-C).

We next sought to further assess the effects of EHD1-KO on CSF-1R ligand-induced activation, signalling, and activation of the MAPK pathway—a well-known driver of proliferation [44,45]. We noted the total CSF-1R levels before and after stimulation were lower in CSF1-deprived EHD1-KO vs. control BMDMs (Fig. 1D and 1F; 0 time points). Commensurate with diminished total macrophage CSF-1R, accumulation of pERK (Fig. 1D-E). and pCSF-1R (Suppl. Fig. 2A-B) in EHD1-KO BMDMs was significantly lower than in control BMDMs.

3.2 EHD1-KO BMDMs have decreased spreading and migration

As stimulation through CSF-1R is known to correlate with rapid macrophage spreading [46], we next examined the impact of EHD1 deletion on this cellular response. BMDMs grown

without (Control) or with (EHD1-KO) TAM were deprived of CSF-1 for 16 hours and then were stimulated with CSF-1 for 10 minutes, fixed, and stained for actin to assess the extent of cell spreading. EHD1-KO BMDMs exhibited reduced spreading in response to CSF-1 stimulation (Fig. 2A-B). We next assessed the impact of EHD1 deletion on CSF1-induced trans-well migration, a well-established response to CSF-1R stimulation [47]. Compared to control, EHD1-KO BMDMs showed a significant reduction in migration (Fig. 2C-D). These data suggest EHD1 positively regulates macrophage spreading and migration through modulation of CSF-1R signalling.

3.3 Expression of cell surface CSF-1R is reduced in EHD1-deficient macrophages

Given the deficits in macrophage functional responses to CSF-1R stimulation (*i.e.,* proliferation, spreading, and migration), we next sought to investigate the expression of CSF-1R at the cell surface in Control and EHD1-KO BMDMs. As BMDMs require the continuous presence of CSF-1 *in vitro*, surface levels of CSF-1R are low under steady state conditions due to continuous receptor activation and lysosomal trafficking of surface CSF-1R [15,24]. Therefore, we assessed the cell surface CSF-1R levels by flow cytometry after 2, 4, 8 or 16 hours of ligand deprivation from the culture medium (CSF-1 deprivation) to allow newly synthesized CSF-1R to accumulate at the cell surface. Initially low CSF-1R surface levels increased steadily over time in Control BMDMs, however cell surface CSF-1R in EHD1-KO BMDMs accumulated at a significantly lower rate. Surface expression of CSF-1R was significantly less at all-time points following CSF-1 deprivation, compared to control cells (Fig. 3A-B). Thus, loss of EHD1 leads to reduced CSF-1R present at the cell surface in BMDMs available for activation by CSF-1.

3.4 Total CSF-1R expression is reduced in EHD1-KO BMDMs

To investigate the mechanism responsible for reduced cell surface expression of CSF-1R on EHD1-KO BMDMs, we first examined the accumulation of total cellular CSF-1R protein after CSF-1was removed from the culture medium using western blotting. $Ehd1^{fl/fl}$; Cre^{ERT2} BMDMs grown in CSF1-containing medium without (Control) or with (EHD1-KO) TAM were switched to medium without CSF-1 for 2, 4, 8 or 16 hours, and cellular lysates were analyzed by immunoblotting for CSF-1R. EHD1-KO BMDMs showed a significant and substantial reduction in the total CSF-1R protein levels at each time point (Fig. 3C-D). These findings indicate that total CSF-1R protein levels are dependent on the presence of EHD1 in the cell.

3.5 EHD1 is required for the display of CSF-1R on the macrophage cell surface

Given the reduction in surface and total CSF-1R in EHD1-KO BMDMs, we carried out qRT-PCR analysis to assess the levels of CSF-1R mRNA expression in control and EHD1-KO BMDMs. $Ehd1^{fl/fl}$; Cre^{ERT2} BMDMs cultured with (Control) or without (EHD1-KO) TAM were harvested under steady state culture conditions or after 16 hours CSF-1 deprivation. CSF-1R mRNA levels increased nearly 50% in CSF-1 deprived control BMDMs compared to control BMDMs cultured under steady-state conditions. Likewise, CSF-1R mRNA levels in CSF-1 deprived EHD1-KO BMDMs increased in a similar pattern to control BMDMs and no significant difference in CSF-1R mRNA expression was observed between control and EHD1-KO BMDMs under steady state or ligand deprived conditions (Fig. 4A). These data

demonstrate that the reduction in surface and total CSF-1R levels in EHD1-KO BMDMs is not due to decreased CSF-1R mRNA expression.

In order to assess if EHD1 deletion affects CSF-1R protein synthesis and/or its post-translational maturation and transport to the cell surface, we preformed metabolic pulse-labeling of the receptor with [^{35}S]-methionine/cysteine followed by chase in CSF1-containing culture medium. Under these conditions, newly synthesized and mature (i.e., glycosylated) CSF-1R that reaches the cell surface is expected to bind to CSF-1 and be targeted for degradation in the lysosome, resulting in a reduction in radioactive signals of mature CSF-1R protein at later time points of chase. Equal quantities of lysates collected at various time points were subjected to anti-CSF-1R immunoprecipitation followed by autoradiography to visualize the immature and mature CSF-1R polypeptides. The signals of immature CSF-1R synthesized during pulse-labeling (time 0) were comparable between control and EHD1-KO BMDMs (Fig. 4B; lower band), thus excluding any alteration in the rate of protein synthesis as the determinant of reduced total CSF-1R levels in EHD1-KO cells observed by Western blot (Fig. 3C-D). Analysis at various times during chase showed that the conversion of immature CSF-1R to a fully glycosylated protein at a greater molecular weight [12] was similar in control and EHD1-KO BMDMs with the majority of immature protein being converting to the mature form by 30 min of chase (Fig. 4B). Notably, mature CSF-1R signals in control BMDMs were clearly diminished by 60 min of chase, reflecting the receptor's arrival at the cell surface and subsequent CSF1-induced internalization and degradation (Fig. 4B) [21]. In contrast, the mature CSF-1R signals remained prominent, and nearly unaltered, at 60 min of chase in EHD1-KO BMDMs (Fig. 4B), indicating a block in CSF-1R receptor trafficking occurs after glycosylation in the Golgi but before ligand-induced internalization and lysosomal degradation. Given the observation that display of CSF-1R at the cell surface is decreased, these data support the conclusion that in EHD1-KO BMDMs the block in CSF-1R receptor trafficking occurs during the stage of receptor transport from the Golgi to the cell surface. In summary, these findings indicate that transcription, translation, and post-translational modification of CSF-1R are unaltered in EHD1-KO macrophages and that EHD1 is required for the transport of CSF-1R to the cell surface after receptor glycosylation in the Golgi.

3.6 A pool of CSF-1R localized to a EHD1$^+$/GM130$^+$ compartment

Given the results of pulse-chase analyses, we asked if EHD1 co-localizes with CSF-1R at the Golgi apparatus. Three-color confocal imaging was performed on fixed and permeabilized control and EHD-KO BMDMs deprived of CSF-1 for 2, 4, 8, and 16 hours to allow for CSF-1R synthesis and accumulation. In control BMDMs, EHD1 strongly co-localized with the Golgi marker GM130 and a pool of CSF-1R localized to this EHD1$^+$/GM130$^+$ compartment (Fig. 5). No EHD1 staining was detected in TAM-induced EHD1-KO BMDMs (Fig. 5). EHD1-KO BMDMs also exhibited a pool of CSF-1R localized to the GM130$^+$ Golgi compartment, with diminished CSF-1R signals near the cell surface (Fig 5). Together with the results of the metabolic pulse-chase (Fig. 4B), these data support the conclusion that EHD1 is involved in directing Golgi-localized CSF-1R to the cell surface, and that in EHD1-KO BMDMs CSF-1R may transit to a different, potentially degradative, cellular compartment.

3.7 CSF-1R is shunted to the lysosome in EHD1-KO BMDMs and results in receptor degradation

To investigate CSF-1R degradation, *Ehd1*$^{fl/fl}$; *Cre*^{ERT2} BMDMs cultured in the absence (control) or presence (EHD1-KO) of TAM were deprived of CSF-1 for 4 hours either in the absence or presence of lysosomal proton pump blocker Bafilomycin A1 (Baf-A1). Western blot analysis demonstrated lower accumulated levels of total CSF-1R protein in EHD1-KO macrophages compared to control when cultured in the absence of Baf-A1 (Fig. 6A-B; 1st and 3rd lanes and Fig. 3C-D). In contrast, inclusion of Baf-A1 led to a dramatic and statistically significant increase in CSF-1R levels in EHD1-KO BMDMs when compared with EHD1-KO BMDMs cultured in the absence of Baf-A1, and nearly approached the levels in control +Baf-A1 BMDMs (Fig. 6A-B). These results suggest that CSF-1R rapidly transits from the Golgi to the lysosome in EHD1-KO BMDMs and results in receptor degradation (Fig. 6A-B). Moreover, increased degradation of CSF-1R (without change in CSF-1R synthesis) in EHD1-KO BMDMs provides a mechanistic explanation for our findings that EHD1-KO macrophages have decreased CSF-1R surface and total levels.

To further demonstrate that CSF-1R is shunted to the lysosome, we carried out confocal imaging of control vs. EHD1-KO BMDMs deprived of CSF-1 for 4 hours in the presence of Baf-A1 and stained for CSF-1R and the lysosomal marker LAMP1. In contrast to a small pool of CSF-1R that localized in LAMP1^{+} lysosomes in control BMDMs, a significantly larger pool of CSF-1R co-localized to LAMP1^{+} lysosomes in EHD1-KO BMDMs (Fig. 6C-D). Overall, these results support the role of EHD1 in the transport of newly synthesized CSF-1R from the Golgi to the macrophage cell surface. Collectively, these data suggest EHD1 governs CSF-1R signalling via control of CSF-1R presentation on the macrophage cell surface.

4. Discussion

CSF-1R is essential for the development and varied functions of monocyte-macrophage lineage cells [2]. Abnormal CSF-1R-dependent macrophage functions contribute to variety of human diseases and aberrant CSF-1R signalling is a contributor to oncogenesis [3,11,48,49]. A pre-requisite for all CSF-1R-mediated macrophage biological functions is the display of the receptor at the cell surface in order for ligand to bind and initiate signal transduction cascades. Mechanisms that govern the post-synthesis/maturation traffic of CSF-1R to the cell surface are therefore biologically pivotal, yet nothing is known about these mechanisms at the present time. Here, we used primary bone marrow-derived macrophages (BMDMs) derived from an inducible knockout mouse model to provide evidence that EHD1, a member of the EHD family of endocytic recycling regulators, serves a novel and critical role in ensuring Golgi to cell surface traffic of CSF-1R. We show that this novel function of EHD1 in delivering CSF-1R from the Golgi to the membrane. In the absence of EHD1, CSF-1R is shunted to the lysosome. Our studies show that EHD1-dependent cell surface transport of CSF-1R ensures subsequent ligand-induced cellular activation. Our findings that EHD1 functions as a novel regulator CSF-1R transport to the cell surface help assign a new functional role to EHD1.

As much of the functional biology of EHD proteins has emerged in the context of non-signalling receptors, we envisioned a potential role of EHD1 in the traffic of the RTK CSF-1R in the absence of its ligand induced trafficking. CSF-1R binding to CSF-1 has been established to induce rapid internalization and lysosomal degradation [16] of the activated receptor, such that surface and total levels of CSF-1R in BMDMs cultured in the continual presence of CSF-1 (steady state) are relatively low. By deliberately examining the levels of surface and total CSF-1R after switching BMDMs from steady-state to CSF-1deprived culture medium, our studies directly focused on the accumulation and traffic of newly synthesized CSF-1R. Analyses of the cell surface and total CSF-1R protein under these conditions, using a combination of flow cytometry (Fig. 3A-B) western blotting (Fig. 3C-D), metabolic pulse-chase (Fig. 4B) and immunofluorescence imaging of non-permeabilized (Suppl. Fig. 3A-B) or permeabilized (Suppl. Fig. 3C-D) BMDMs demonstrated a clear impairment in the ability of newly synthesized CSF-1R to be transported to the cell surface and an overall reduction in CSF-1R levels when EHD1 was deleted.

Previous studies have shown that reduced surface expression of CSF-1R can result from defective glycosylation. This is seen upon expression of the HIV protein NEF, which inhibits glycosylation through an incompletely understood mechanism involving NEF activation of the SRC-family tyrosine kinase HCK as well as through an HCK-independent mechanism [50,51]. Naturally-occurring loss-of-function mutations of CSF-1R have been identified in patients with hereditary diffuse leukoencephalopathy with spheroids (HDLS), and most of these mutations result in reduced CSF-1R protein expression [8]. In both of the aforementioned cases, CSF-1R glycosylation in the Golgi is defective. In contrast, our metabolic pulse-chase studies (Fig. 4B) showed that immature CSF-1R was fully converted into a mature form (fully glycosylated with higher molecular weight) in EHD1-KO BMDMs with essentially the same kinetics as in control cells. These findings clearly pointed to the possibility that post-synthetic transport of CSF-1R after its Golgi processing was defective in EHD1-KO BMDMs. Consistent with this idea, we observed that CSF-1R co-localizes Golgi marker GM130 (Fig. 5). Our metabolic pulse-chase studies carried out in the presence of CSF-1 exposed the newly synthesized CSF-1R to its ligand, which promoted its rapid degradation. While this was clearly seen in control BMDMs, the mature band of CSF-1R remained intact for the duration of the experiment in EHD1-KO BMDMs (Fig. 4B), supporting the conclusion that ^{35}S-labled CSF-1R did not reach the cell surface, consistent with results from flow cytometry (Fig. 3A-B) and immunofluorescence microscopy (Suppl. Fig. 3A-B) analyses. When combined with the observed reduction in total CSF-1R levels in EHD1-KO BMDMs, these results led us to hypothesize that lack of EHD1 allows CSF-1R traffic from the Golgi to a compartment where it is degraded. As RTKs are known to be degraded in lysosomes [15,22] and a variety of receptors are known to traffic from the Golgi to the lysosome directly [52,53], we considered the possibility that in EHD1-KO BMDMs CSF-1R is alternatively sorted to the lysosome and subsequently degraded. Our Western blotting analyses demonstrating that CSF-1R protein accumulates in EHD1-KO BMDMs when cultured in the presence of Baf-A1 (Fig. 6A-B), together with confocal imaging of Baf-A1 treated BMDMs (Fig. 6C-D) support this mechanism.

It is of obvious interest to assess if the EHD1-dependent CSF-1R transport pathway we describe is also important for other RTKs or represents a more restricted adaptation for

CSF-1R. How the balance of these pathway operates and whether it is tunable during development, differentiation or functional responses of macrophage-lineage or other cells will be of great interest, especially in the context of human diseases in which inhibition of CSF-1R signalling would be desirable [3,9,54,55].

5. Conclusions

In summary, our data suggest that exit of fully glycosylated and mature CSF-1R from the Golgi is a regulated process under the control of two competing sorting processes: a dominant EHD1-dependent pathway to facilitate traffic to the cell surface and an alternate pathway of traffic to lysosomes for degradation. Our findings support the conclusion that EHD1-dependent CSF-1R sorting decisions at the Golgi are of key significance in determining the ultimate level of CSF-1R signalling and downstream biological responses.

Supplementary Material

Refer to Web version on PubMed Central for supplementary material.

Acknowledgments

This work was supported by: the NIH grants CA105489, CA87986, CA99163 and CA116552 to HB, CA105489-supplement to FI and CA96844 and CA144027 to VB; Department of Defense grants W81XWH-07-1-0351 and W81XWH-11-1-0171 (VB); the NE DHHS LB-506 (2014-01) and LB606 (18123-Y3) grants (HB); Institutional Development Award (IDeA) from the NIGMS of the NIH under grant number P30 GM106397. The UNMC Confocal, Flow Cytometry and other Core facilities from the NCI Cancer Center Support Grant (P30CA036727) to Fred & Pamela Buffett Cancer Center and the Nebraska Research Initiative.

LC and TB are trainees under the NCI Cancer Biology Training Grant (T32CA009476). WA was a recipient of a UNMC graduate fellowship.

We thank Garland (Michael) Upchurch for insight, suggestions, and critical reading/proofing of the manuscript.

Abbreviations

CSF1R	Colony Stimulating Factor 1 Receptor
CSF1	Colony Stimulating Factor-1
BMDM	Bone Marrow Derived Macrophage
EHD1	Eps-15 Homology Domain-containing protein 1
EHD1-KO	EHD1-KnockOut (4-hydroxytamoxifen induced deletion)
RTK	Receptor Tyrosine Kinase
TAM	4-Hydroxytamoxifen
FACS	Fluorescence Activated Cell Sorting
c.p.m.	counts per minute
GM130	Golgi Matrix Protein (130kD)

LAMP1	Lysosomal associated membrane protein 1
PFA	Paraformaldehyde
BSA	Bovine Serum Albumin

References

1. Jenkins SJ, Hume DA. Homeostasis in the mononuclear phagocyte system. Trends Immunol. 2014; 35:358–367. doi:10.1016/j.it.2014.06.006. [PubMed: 25047416]
2. Hume DA. Differentiation and heterogeneity in the mononuclear phagocyte system. Mucosal Immunol. 2008; 1:432–441. doi:10.1038/mi.2008.36. [PubMed: 19079210]
3. Chitu V, Stanley ER. Colony-stimulating factor-1 in immunity and inflammation. Curr. Opin. Immunol. 2006; 18:39–48. doi:10.1016/j.coi.2005.11.006. [PubMed: 16337366]
4. Hamilton JA. Colony-stimulating factors in inflammation and autoimmunity John. Nat. Immunol. 2008; 23:533–544. doi:10.1016/S1471-4906(02)02260-3.
5. Pollard JW. Trophic macrophages in development and disease. Nat. Rev. Immunol. 2009; 9:259–70. doi:10.1038/nri2528. [PubMed: 19282852]
6. Toh ML, Bonnefoy JY, Accart N, Cochin S, Pohle S, Haegel H, et al. Bone- and cartilage-protective effects of a monoclonal antibody against colony-stimulating factor 1 receptor in experimental arthritis. Arthritis Rheumatol. 2014; 66:2989–3000. doi:10.1002/art.38624. [PubMed: 24623505]
7. Bogie JFJ, Stinissen P, Hendriks JJA. Macrophage subsets and microglia in multiple sclerosis. Acta Neuropathol. 2014; 128:191–213. doi:10.1007/s00401-014-1310-2. [PubMed: 24952885]
8. Sundal C, Fujioka S, Van Gerpen JA, Wider C, Nicholson AM, Baker M, et al. Parkinsonian features in hereditary diffuse leukoencephalopathy with spheroids (HDLS) and CSF1R mutations. Park. Relat. Disord. 2013; 19:869–877. doi:10.1016/j.parkreldis.2013.05.013.
9. Aikawa Y, Katsumoto T, Zhang P, Shima H, Shino M, Terui K, et al. PU.1-mediated upregulation of CSF1R is crucial for leukemia stem cell potential induced by MOZ-TIF2. Nat. Med. 2010; 16:580–585. 1p following 585. doi:10.1038/nm.2122. [PubMed: 20418886]
10. Qian B-Z, Li J, Zhang H, Kitamura T, Zhang J, Campion LR, et al. CCL2 recruits inflammatory monocytes to facilitate breast-tumour metastasis. Nature. 2011; 475:222–5. doi:10.1038/nature10138. [PubMed: 21654748]
11. Laoui D, van Overmeire E, de Baetselier P, van Ginderachter JA, Raes G. Functional relationship between tumor-associated macrophages and macrophage colony-stimulating factor as contributors to cancer progression. Front. Immunol. 2014; 5:1–15. doi:10.3389/fimmu.2014.00489. [PubMed: 24474949]
12. Pixley FJ, Stanley ER. CSF-1 regulation of the wandering macrophage: Complexity in action. Trends Cell Biol. 2004; 14:628–638. doi:10.1016/j.tcb.2004.09.016. [PubMed: 15519852]
13. Wei S, Nandi S, Chitu V, Yeung Y-GY-G, Yu W, Huang M, et al. Functional overlap but differential expression of CSF-1 and IL-34 in their CSF-1 receptor-mediated regulation of myeloid cells. J. Leukoc. Biol. 2010; 88:495–505. doi:10.1189/jlb.1209822. [PubMed: 20504948]
14. Liu H, Leo C, Chen X, Wong BR, Williams LT, Lin H, et al. The mechanism of shared but distinct CSF-1R signaling by the non-homologous cytokines IL-34 and CSF-1. Biochim. Biophys. Acta - Proteins Proteomics. 2012; 1824:938–945. doi:10.1016/j.bbapap.2012.04.012.
15. Lee PSW, Wang Y, Dominguez MG, Yeung YG, Murphy MA, Bowtell DDL, et al. The Cbl protooncoprotein stimulates CSF-1 receptor multiubiquitination and endocytosis, and attenuates macrophage proliferation. EMBO J. 1999; 18:3616–3628. doi:10.1093/emboj/18.13.3616. [PubMed: 10393178]
16. Wang Y, Yeung YG, Langdon WY, Stanley ER. c-Cbl is transiently tyrosinephosphorylated, ubiquitinated, and membrane-targeted following CSF-1 stimulation of macrophages. J. Biol. Chem. 1996; 271:17–20. doi:10.1074/jbc.271.1.17. [PubMed: 8550554]
17. Xiong Y, Song D, Cai Y, Yu W, Yeung YG, Stanley ER. A CSF-1 receptor phosphotyrosine 559 signaling pathway regulates receptor ubiquitination and tyrosine phosphorylation. J. Biol. Chem. 2011; 286:952–960. doi:10.1074/jbc.M110.166702. [PubMed: 21041311]

18. Mohapatra B, Ahmad G, Nadeau S, Zutshi N, An W, Scheffe S, et al. Protein tyrosine kinase regulation by ubiquitination: Critical roles of Cbl-family ubiquitin ligases. Biochim. Biophys. Acta. 2013; 1833:122–139. doi:10.1016/j.bbamcr.2012.10.010. [PubMed: 23085373]
19. Ahmad G, Mohapatra BC, Schulte NA, Nadeau SA, Luan H, Zutshi N, et al. Cbl-family ubiquitin ligases and their recruitment of CIN85 are largely dispensable for epidermal growth factor receptor endocytosis. Int. J. Biochem. Cell Biol. 2014; 57:123–134. doi:10.1016/j.biocel.2014.10.019. [PubMed: 25449262]
20. Miyake S, Lupher ML, Druker B, Band H. The tyrosine kinase regulator Cbl enhances the ubiquitination and degradation of the platelet-derived growth factor receptor alpha. Proc. Natl. Acad. Sci. U. S. A. 1998; 95:7927–32. doi:10.1073/pnas.95.14.7927. [PubMed: 9653117]
21. Wang Y, Yeung YG, Stanley ER. CSF-1 stimulated multiubiquitination of the CSF-1 receptor and of Cbl follows their tyrosine phosphorylation and association with other signaling proteins. J. Cell. Biochem. 1999; 72:119–134. doi:10.1002/(SICI)1097-4644(19990101)72:1<119::AID-JCB13>3.0.CO;2-R. [PubMed: 10025673]
22. Goh LLK, Sorkin A. Endocytosis of receptor tyrosine kinases. Cold Spring Harb. Perspect. 2013; 5:a017459. doi:10.1101/cshperspect.a017459.
23. Huynh J, Kwa MQ, Cook AD, Hamilton JA, Scholz GM. CSF-1 receptor signalling from endosomes mediates the sustained activation of Erk1/2 and Akt in macrophages. Cell. Signal. 2012; 24:1753–1761. doi:10.1016/j.cellsig.2012.04.022. [PubMed: 22575736]
24. Guilbert LJ, Stanley ER. The interaction of 125I-colony-stimulating factor-1 with bone marrow-derived macrophages. J. Biol. Chem. 1986; 261:4024–4032. [June 19, 2015] http://www.ncbi.nlm.nih.gov/pubmed/3485098. [PubMed: 3485098]
25. Naslavsky N, Caplan S. EHD proteins: key conductors of endocytic transport. Trends Cell Biol. 2010; 21:122–131. doi:10.1016/j.tcb.2010.10.003. [PubMed: 21067929]
26. Grant BD, Caplan S. Mechanisms of EHD/RME-1 protein function in endocytic transport. Traffic. 2008; 9:2043–2052. doi:10.1111/j.1600-0854.2008.00834.x. [PubMed: 18801062]
27. Daumke O, Lundmark R, Vallis Y, Martens S, Butler PJG, McMahon HT. Architectural and mechanistic insights into an EHD ATPase involved in membrane remodelling. Nature. 2007; 449:923–7. doi:10.1038/nature06173. [PubMed: 17914359]
28. Posey AD, Pytel P, Gardikiotes K, Demonbreun AR, Rainey M, George M, et al. Endocytic recycling proteins EHD1 and EHD2 interact with Fer-1-like-5 (Fer1L5) and mediate myoblast fusion. J. Biol. Chem. 2011; 286:7379–7388. doi:10.1074/jbc.M110.157222. [PubMed: 21177873]
29. Posey AD, Swanson KE, Alvarez MG, Krishnan S, Earley JU, Band H, et al. EHD1 mediates vesicle trafficking required for normal muscle growth and transverse tubule development. Dev. Biol. 2014; 387:179–190. doi:10.1016/j.ydbio.2014.01.004. [PubMed: 24440153]
30. George M, Rainey MA, Naramura M, Foster KW, Holzapfel MS, Willoughby LL, et al. Renal thrombotic microangiopathy in mice with combined deletion of endocytic recycling regulators EHD3 and EHD4. PLoS One. 2011; 6:e17838. doi:10.1371/journal.pone.0017838. [PubMed: 21408024]
31. Curran J, Makara MA, Little SC, Musa H, Liu B, Wu X, et al. EHD3-dependent endosome pathway regulates cardiac membrane excitability and physiology. Circ. Res. 2014; 115:68–78. doi:10.1161/CIRCRESAHA.115.304149. [PubMed: 24759929]
32. Curran J, Musa H, Kline CF, Makara MA, Little SC, Higgins JD, et al. Eps15 homology domain-containing protein 3 regulates cardiac T-type Ca^{2+} channel targeting and function in the atria. J. Biol. Chem. 2015; 290:12210–12221. doi:10.1074/jbc.M115.646893. [PubMed: 25825486]
33. Gudmundsson H, Curran J, Kashef F, Snyder JS, Smith SA, Vargas-Pinto P, et al. Differential regulation of EHD3 in human and mammalian heart failure. J. Mol. Cell. Cardiol. 2012; 52:1183–1190. doi:10.1016/j.yjmcc.2012.02.008. [PubMed: 22406195]
34. Sengupta S, George M, Miller KK, Naik K, Chou J, Cheatham MA, et al. EHD4 and CDH23 are interacting partners in cochlear hair cells. J. Biol. Chem. 2009; 284:20121–20129. doi:10.1074/jbc.M109.025668. [PubMed: 19487694]
35. George M, Rainey MA, Naramura M, Ying G, Harms DW, Vitaterna MH, et al. Ehd4 is required to attain normal prepubertal testis size but dispensable for fertility in male mice. Genesis. 2010; 48:328–342. doi:10.1002/dvg.20620. [PubMed: 20213691]

36. Arya P, Rainey MA, Bhattacharyya S, Mohapatra BC, George M, Kuracha MR, et al. The endocytic recycling regulatory protein EHD1 Is required for ocular lens development. Dev. Biol. 2015; 408:1–15. doi:10.1016/j.ydbio.2015.10.005.
37. Bhattacharyya S, Rainey MA, Arya P, Dutta S, George M, Storck MD, et al. Endocytic recycling protein EHD1 regulates primary cilia morphogenesis and SHH signaling during neural tube development. Sci. Rep. 2016; 6:20727. doi:10.1038/srep20727. [PubMed: 26884322]
38. Rainey MA, George M, Ying G, Akakura R, Burgess DJ, Siefker E, et al. The endocytic recycling regulator EHD1 is essential for spermatogenesis and male fertility in mice. BMC Dev. Biol. 2010; 10:37. doi:10.1186/1471-213X-10-37. [PubMed: 20359371]
39. Weischenfeldt J, Porse B. Bone marrow-derived macrophages (BMM): Isolation and applications. Cold Spring Harb. Protoc. 2008; 3:pdb.prot5080–pdb.prot5080. doi:10.1101/pdb.prot5080.
40. Schmittgen TD, Livak KJ. Analyzing real-time PCR data by the comparative CT method. Nat. Protoc. 2008; 3:1101–1108. doi:10.1038/nprot.2008.73. [PubMed: 18546601]
41. Bailey TA, Luan H, Tom E, Bielecki TA, Mohapatra B, Ahmad G, et al. A kinase inhibitor screen reveals protein kinase C-dependent endocytic recycling of ErbB2 in breast cancer cells. J. Biol. Chem. 2014; 289:30443–30458. doi:10.1074/jbc.M114.608992. [PubMed: 25225290]
42. Simoncic PD, Bourdeau A, Lee-Loy A, Rohrschneider LR, Tremblay ML, Stanley ER, et al. T-cell protein tyrosine phosphatase (Tcptp) is a negative regulator of colony-stimulating factor 1 signaling and macrophage differentiation. Mol. Cell. Biol. 2006; 26:4149–60. doi:10.1128/MCB.01932-05. [PubMed: 16705167]
43. Stanley ER. Factors regulating macrophage production and growth: identity of colony- stimulating factor and macrophage growth factor. J. Exp. Med. 1976; 143:631–647. doi:10.1084/jem.143.3.631. [PubMed: 1082493]
44. Wimmer R, Baccarini M. Partner exchange: Protein-protein interactions in the Raf pathway. Trends Biochem. Sci. 2010; 35:660–668. doi:10.1016/j.tibs.2010.06.001. [PubMed: 20621483]
45. Liao RS, Ma S, Miao L, Li R, Yin Y, Raj GV. Androgen receptor-mediated nongenomic regulation of prostate cancer cell proliferation. Transl. Androl. Urol. 2013; 2:187–196. doi:10.3978/j.issn.2223-4683.2013.09.07. [PubMed: 26816736]
46. Yeung YG, Stanley ER. Proteomic Approaches to the Analysis of Early Events in Colony-stimulating Factor-1 Signal Transduction. Mol.Cell Proteomics. 2003; 2:1143–1155. doi:10.1074/mcp.R300009-MCP200. [PubMed: 12966146]
47. Pixley FJ. Macrophage migration and its regulation by CSF-1. Int. J. Cell Biol. 2012; 2012:501962. doi:10.1155/2012/501962. [PubMed: 22505929]
48. Hume DA, MacDonald KPA. Therapeutic applications of macrophage colony-stimulating factor-1 (CSF-1) and antagonists of CSF-1 receptor (CSF-1R) signaling. Blood. 2012; 119:1810–1820. doi:10.1182/blood-2011-09-379214. [PubMed: 22186992]
49. Jeffery JJ, Lux K, Vogel JS, Herrera WD, Greco S, Woo H-H, et al. Autocrine inhibition of the c-fms proto-oncogene reduces breast cancer bone metastasis assessed with in vivo dual-modality imaging. Exp. Biol. Med. 2014; 239:404–413. doi:10.1177/1535370214522588.
50. Hassan R, Suzu S, Hiyoshi M, Takahashi-Makise N, Ueno T, Agatsuma T, et al. Dys-regulated activation of a Src tyroine kinase Hck at the Golgi disturbs N-glycosylation of a cytokine receptor Fms. J. Cell. Physiol. 2009; 221:458–468. doi:10.1002/jcp.21878. [PubMed: 19585521]
51. Hiyoshi M, Suzu S, Yoshidomi Y, Hassan R, Harada H, Sakashita N, et al. Interaction between Hck and HIV-1 Nef negatively regulates cell surface expression of M-CSF receptor. Blood. 2008; 111:243–250. doi:10.1182/blood-2007-04-086017. [PubMed: 17893228]
52. Gomez TS, Gorman J. a. Artal-Martinez de Narvajas a. Koenig a. O. Billadeau DD. Trafficking defects in WASH-knockout fibroblasts originate from collapsed endosomal and lysosomal networks. Mol. Biol. Cell. 2012; 23:3215–3228. doi:10.1091/mbc.E12-02-0101. [PubMed: 22718907]
53. Tu C, Ortega-Cava CF, Chen G, Fernandes ND, Cavallo-Medved D, Sloane BF, et al. Lysosomal cathepsin B participates in the podosome-mediated extracellular matrix degradation and invasion via secreted lysosomes in v-Src fibroblasts. Cancer Res. 2008; 68:9147–9156. doi:10.1158/0008-5472.CAN-07-5127. [PubMed: 19010886]

54. Strachan DC, Ruffell B, Oei Y, Bissell MJ, Coussens LM, Pryer N, et al. CSF1R inhibition delays cervical and mammary tumor growth in murine models by attenuating the turnover of tumor-associated macrophages and enhancing infiltration by CD8(+) T cells. Oncoimmunology. 2013; 2:e26968. doi:10.4161/onci.26968. [PubMed: 24498562]

55. Hernandez L, Smirnova T, Kedrin D, Wyckoff J, Zhu L, Stanley ER, et al. The EGF/CSF-1 paracrine invasion loop can be triggered by heregulin ß1 and CXCL12. Cancer Res. 2009; 69:3221–3227. doi:10.1158/0008-5472.CAN-08-2871. [PubMed: 19293185]

Highlights

- CSF-1R transport and display at the cell surface have not been studied in depth.
- A novel function for EHD1 in anterograde trafficking of CSF-1R was discovered.
- EHD1 was found to be essential for CSF-1R presentation on the macrophage cell surface.
- Targeting of CSF-1R presentation to the cell surface may improve diseases in which CSF-1R signalling is aberrant.

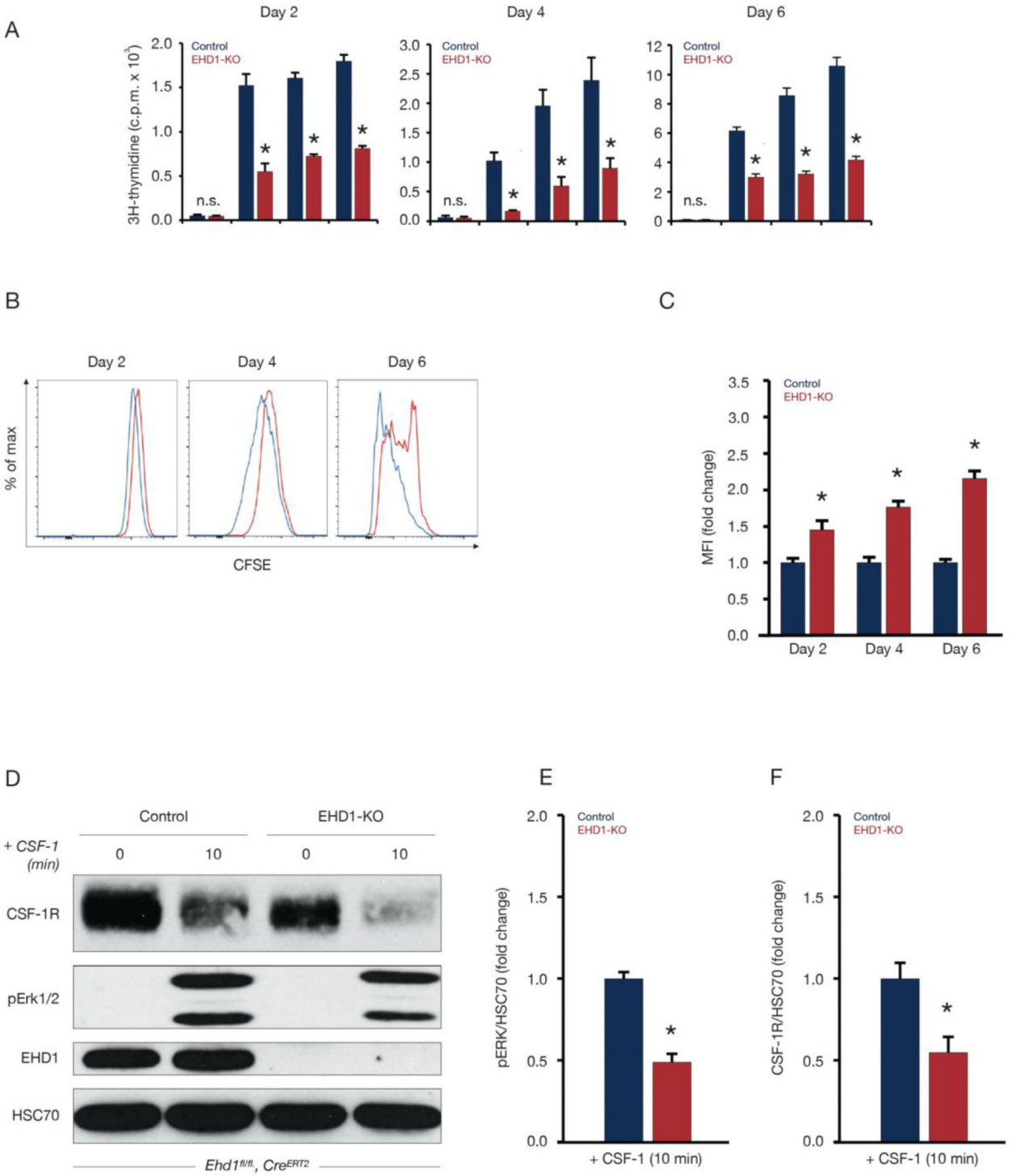

Fig. 1.

CSF-1R signalling and proliferation in Control and EHD1-KO BMDMs. (A) BMDM proliferation as measured by ^{3}H-thymidine incorporation. *Ehd1*$^{fl/fl}$; *Cre*^{ERT2} BMDMs cultured without (Control) or with (EHD1-KO) TAM were stimulated with CSF-1 at 0, 15, 30 or 60 ng/ml for 2, 4 or 6 days. (B) BMDM proliferation as measured by CFSE dye dilution assay. Control and EHD1-KO BMDMs were stained with CFSE dye (day 0) and subsequently stimulated with 30 ng/ml recombinant CSF-1 for 2, 4, or 6 days. (C) Quantification of CFSE Mean Fluorescence Intensity (MFI) Fig. 1B. MFI fold change was

normalized relative to Control BMDMs. (D) Western blot for total CSF-1R and pERK levels after 10 minutes CSF-1 stimulation in Control and EHD1-KO BMDMs. Control and EHD1-KO BMDMs deprived of CSF-1 for 16 hours and then stimulated for 10 minutes with 100 ng/mL CSF-1. 40 μg aliquots of protein lysate were immunoblotted for the indicated antibodies. (E) The relative levels of pERK signals were normalized to HSC70 and expressed at a fold change by defining pERK levels in Control BMDMs as 1. (F) The relative levels of total CSF-1R signals were normalized to HSC70 and expressed at a fold change by defining total CSF-1R levels in Control BMDMs +CSF-1 (10min) as 1. Data from three independent experiments are presented as the mean ± SEM (*=$p<0.05$).

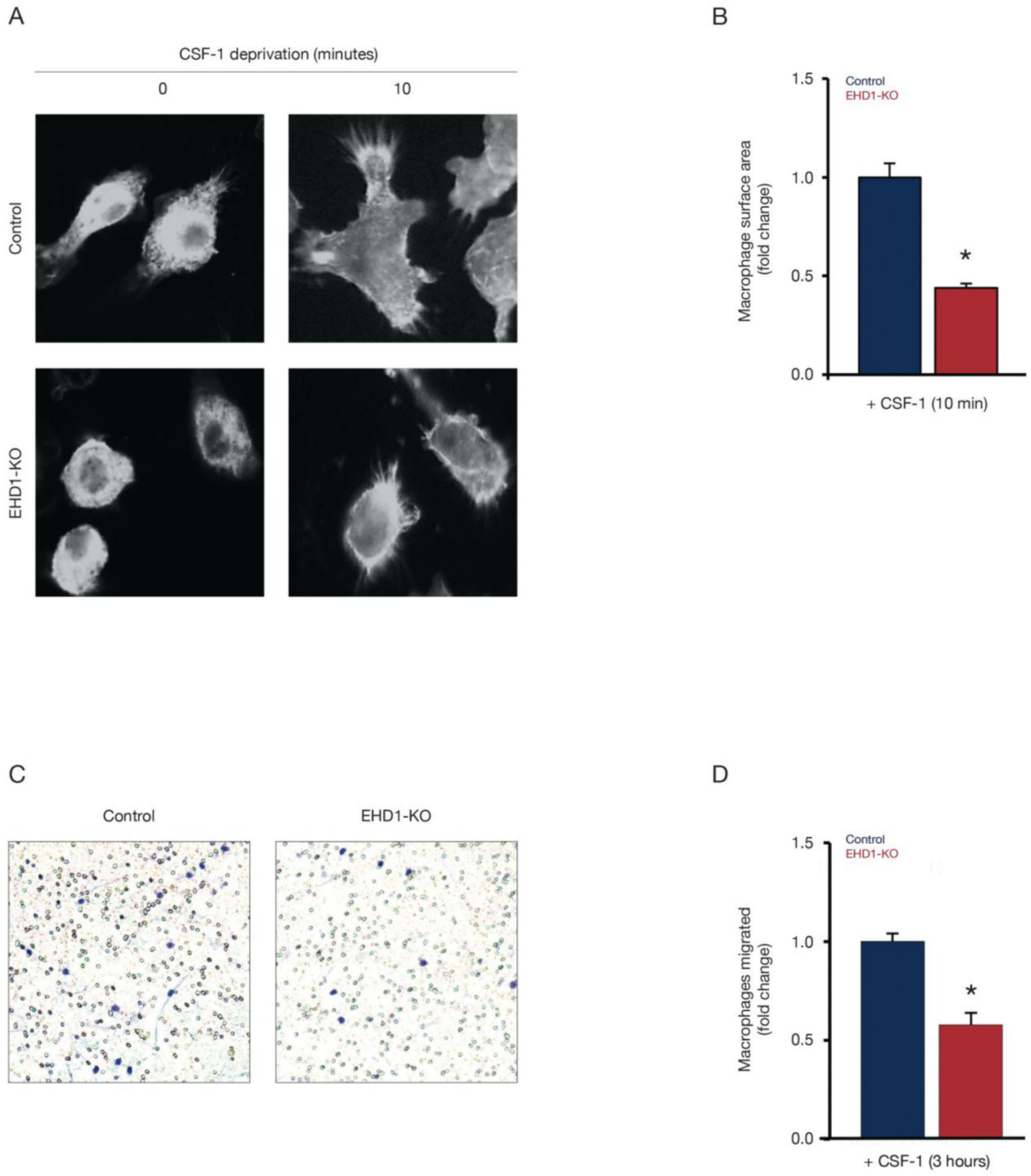

Fig. 2.

Spreading and migration in Control and EHD1-KO BMDMS. (A) Microscopy analysis of macrophage cell surface area after 10 minutes CSF-1 stimulation to assess cell spreading. *Ehd1*$^{fl/fl}$; *Cre*^{ERT2} BMDMs cultured without (Control) or with (EHD1-KO) TAM were deprived of CSF-1 for 16 hours, stimulated with 100 ng/ml CSF-1 for 10 minutes. Cells were then fixed, permeabilized, stained for polymerized actin using conjugated phalloidin-594, and visualized by confocal microscopy. (B) Quantification of cellular spreading from Fig. 2A was done by analyzing the cell surface area (corresponding to

phalloidin staining) using ImageJ software (n = 100 cells were counted in 3 independent experiments. Cell surface area was normalized to Control BMDMs. (C) Trans-well migration assay. Control and EHD1-KO BMDMs were deprived of CSF-1 for 4 hours and allowed to migrate towards CSF-1 (30 ng/ml) in the lower chamber of Boyden Transwell chambers. Filters were HEMA stained and photographed at 20x. (D) Quantification of migration assay from Fig. 2C. Total cells migrated were normalized to Control BMDMs. Data from three independent experiments are presented as the mean ± SEM (*=$p<0.05$).

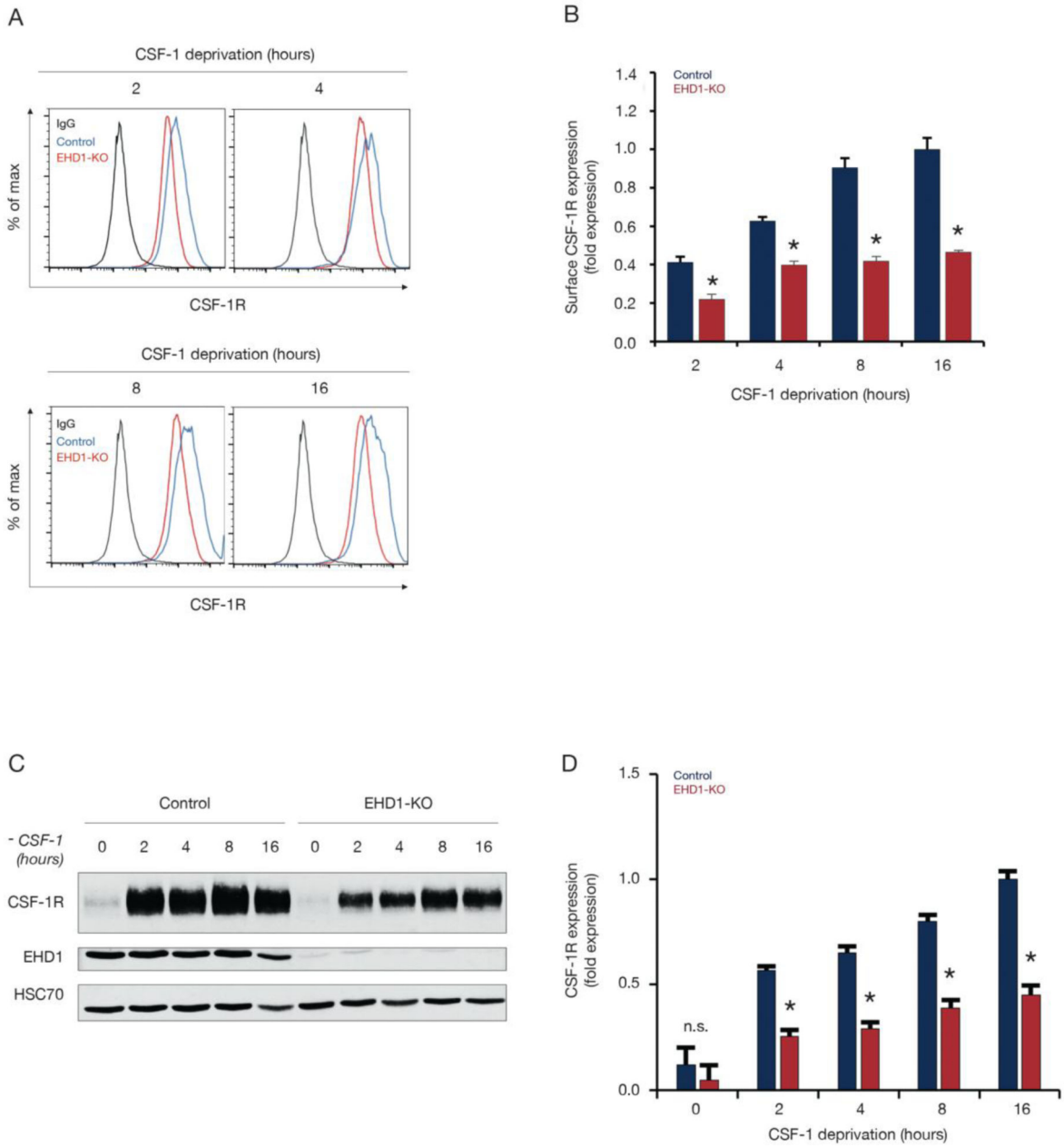

Fig. 3.

Surface CSF-1R expression in Control and EHD1-KO BMDMS after CSF-1 deprivation. (A) Surface CSF-1R staining for analysis via FACS. *Ehd1*$^{fl/fl}$; *Cre*^{ERT2} BMDMs treated without (Control) or with (EHD1-KO) TAM were deprived of CSF-1 for 2, 4, 8, or 16 hours and stained with anti-CSF-1R antibody, then measured by FACS analysis. Grey histograms represent IgG control. (B) Quantification of CSF-1R surface expression from Fig. 3A. Data is presented as the fold change of MFI, with the 16 hour CSF-1 deprivation from Control BMDMs deprived of CSF-1 for 16 hours normalized to 1. (C) Immunoblotting for total CSF-1R expression in Control and EHD1-KO BMDMS after CSF-1 deprivation. *Ehd1*$^{fl/fl}$; *Cre*^{ERT2} BMDMs without (Control) or with (EHD1-KO) TAM were CSF-1 deprived for 2,

4, 8, 16 hours, lysed, and subsequently analyzed by immunoblotting for the indicated antibodies.

(D) Quantification of total CSF-1R protein assessed by western blotting in Fig. 3C. The CSF-1R band pixels were quantified from scanned blots using ImageJ software, normalized by HSC70 intensity, and expressed as a fold change by defining Control BMDMs CSF-1 deprived for 16 hours as 1. Data from three independent experiments are presented as the mean ± SEM (*=$p<0.05$, ***=$p<0.001$, ns = not significant).

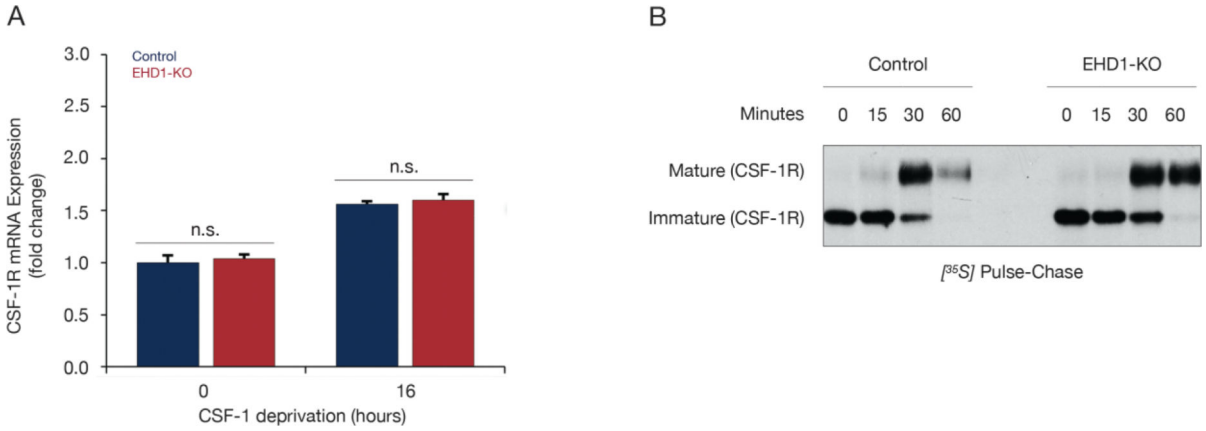

Fig. 4.

CSF-1R protein synthesis or its post-translational maturation in Control and EHD1-KO BMDMs. (A) RNA was isolated from *Ehd1*$^{fl/fl}$; *Cre*^{ERT2} BMDMs without (Control) or with (EHD1-KO) TAM and subsequently deprived of CSF-1 for 0 and 16 hours. CSF-1R mRNA expression was measured by qRTPCR. CSF-1R mRNA expression was normalized by GAPDH and expressed as a fold change by setting Control BMDMs at 0 hours starvation to 1. (B) Metabolic pulse-labelling followed by chase to show unaltered translation and maturation with a block of surface transport of newly synthesized CSF-1R in BMDMs. Control and EHD1-KO BMDMs were metabolically pulse-labeled with [^{35}S] methionine/cysteine for 15 min and subjected to chase in unlabeled methionine/cysteine-enriched medium in the presence of CSF-1 for the indicated times followed by cell lysis. 500 μg aliquots of sample lysates were subjected to anti-CSF-1R immunoprecipitation followed by autoradiography. Lower band represents the immature/non-glycosylated CSF-1R; upper band represents the mature/fully glycosylated CSF-1R. Note the comparable lower band signals at time 0 and similar rates of conversion to the upper band; however, the signals corresponding to the mature upper band are lost in Control BMDMs but remain intact in EHD1-KO BMDMs indicating arrival at the cell surface and ligand-induced degradation. Data from three independent experiments are presented as the mean ± SEM (n.s. = not significant).

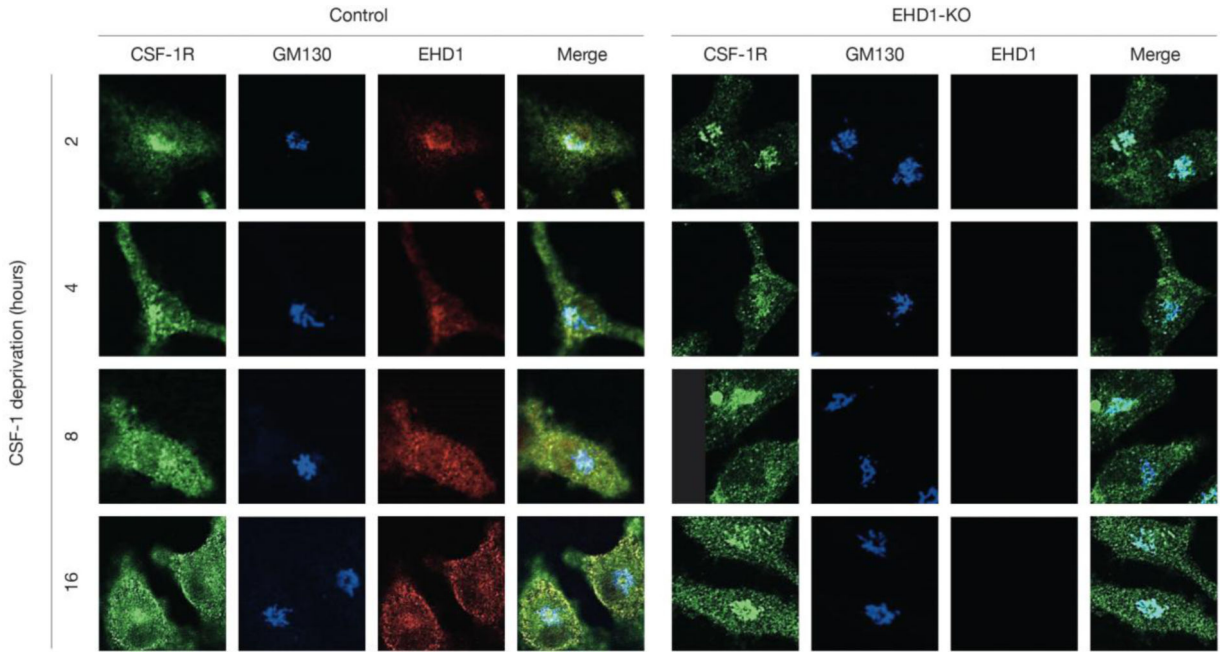

Fig. 5.

CSF-1R, EHD1, and GM130 staining in Control and EHD1-KO BMDMs after CSF-1 deprivation. Confocal immunofluorescence showing co-localization of EHD1 with CSF1R at the Golgi apparatus. *Ehd1*$^{fl/fl}$; *Cre*^{ERT2} BMDMs cultured without (Control) or with (EHD1-KO) TAM were switched from CSF1-containing medium to CSF1-free medium for 2, 4, 8 or 16 hours and subsequently fixed, permeabilized and stained for CSF1R (green), EHD1 (Red) and GM130—Golgi marker (Blue) and analyzed by confocal microscopy. Merged pictures are shown on the right. Representative images from three independent experiments is shown.

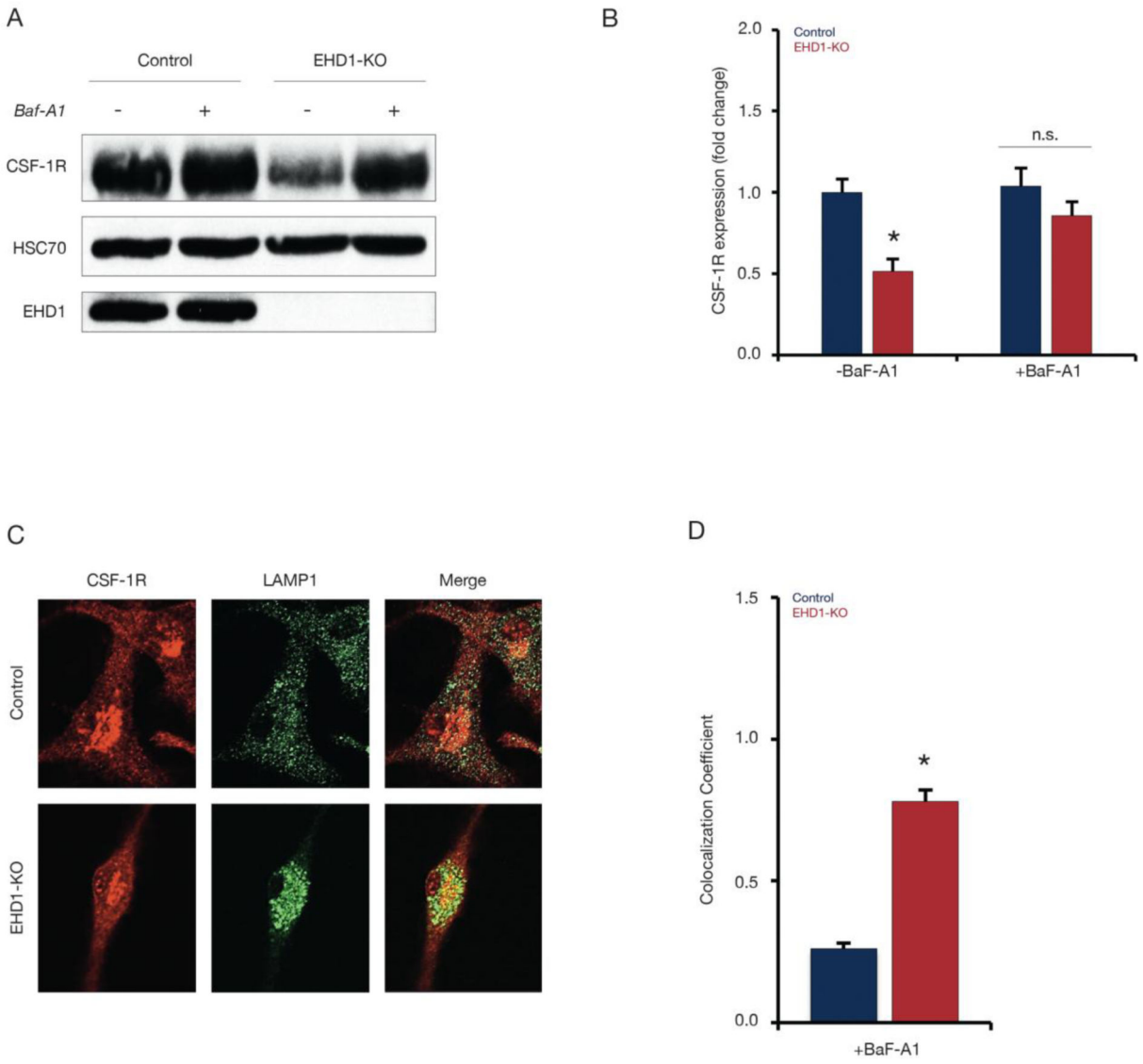

Fig. 6.

Effects of Baf-A1 on total CSF-1R levels in Control and EHD-1KO BMDMs after CSF-1 deprivation. (A) Western blot analysis to show recovery of total CSF-1R levels in EHD1-KO BMDMs upon inhibition of lysosomal degradation. *Ehd1*$^{fl/fl}$; *Cre*^{ERT2} BMDMs treated without (Control) or with (EHD1-KO) TAM were switched from CSF-1-containing medium to CSF-1-free medium for 4 hours in the absence (−Baf-A1) or presence (+Baf-A1) of the lysosomal inhibitor Baf-A1 (100 nM). 40 μg of protein lysates were immunoblotted for total CSF-1R, HSC70 (loading control), and EHD1. (B) Quantification of total CSF-1R signals from Fig. 7A. Data were normalized to HSC70 signals and expressed as a fold change relative to values for Control BMDMs without Baf-A1 treatment (n = 3; *=$p<0.05$; n.s. = not significant). (C) Representative confocal immunofluorescence image showing colocalization of CSF-1R in LAMP1+ lysosomes of EHD1-KO BMDMs after lysosomal inhibition with Baf-A1. Control and EHD1-KO BMDMs from *Ehd1*$^{fl/fl}$; *Cre*^{ERT2} mice were switched from CSF-1-containing to CSF-1-free medium for 4 hours in the presence of 100 nM Baf-A1.

Cells were fixed, permeabilized, and stained for analysis by immunofluorescence: CSF-1R (red) and LAMP1 (green); merged pictures on right show colocalization (yellow). (D) Quantification of CSF-1R and LAMP1 colocalization from Fig. 7C. Colocalization of CSF-1R and LAMP1 fluorescence signals was assessed in 50 cells in 3 independent experiments to determine the colocalization coefficient ± SEM (n = 150, *=$p<0.05$, n.s. = not significant).